

IMPROVED METHODS FOR TIME DOMAIN ELECTROMAGNETIC SOUNDING OF THE MOON. H. Fuqua Haviland¹, A. R. Poppe¹, S. Fatemi², G. T. Delory¹. ¹Space Sciences Laboratory, University of California, Berkeley, CA 94720, (heidi.fuqua@berkeley.edu), ²Swedish Institute of Space Physics.

Introduction: Time Domain Electromagnetic (TDEM) Sounding isolates induced magnetic fields to remotely deduce lunar material properties at depth. The first step of performing TDEM Sounding at the Moon is to characterize the dynamic plasma environment, and to be able to isolate geophysically induced currents from concurrently present plasma currents. The TDEM Sounding transfer function method requires a two-point measurement: an upstream reference measuring the pristine solar wind, and one downstream near the Moon. This method was last performed during Apollo assuming the induced fields on the nightside of the Moon expand as if in an undisturbed vacuum within the wake cavity [1]. TDEM sounding is particularly well suited for measurements from moving satellite platforms directly accounting for changing altitudes [2].

Here, we present an approach for isolating induced fields, thereby improving the accuracy of existing TDEM methods. Our models include a plasma induction model capturing the kinetic plasma environment within the wake cavity around a conducting Moon, and an analytic expression of the geophysical forward model capturing induction in a vacuum. This method can be applied to any two point magnetometer measurement of the Moon or similar airless bodies.

Transient Plasma Induction Model: Plasma hybrid models use the upstream plasma conditions and interplanetary magnetic field (IMF) to capture the wake current systems that form around the Moon. The plasma kinetic equations are solved for particle ions with electrons included as a charge-neutralizing fluid. These models accurately capture the large scale lunar wake dynamics for a variety of solar wind conditions (ion density, temperature, solar wind velocity, and IMF orientation) [3]. Previously, Fatemi et al. (2015) [4] showed that magnetic fields representative of induction are not confined within the wake cavity according to the wake-induced field interaction. Given the 3D orientation variability coupled with the large range of solar wind conditions seen within the lunar plasma environment, we must understand the environment one case at a time. Here, we use a GPU-based three-dimensional hybrid model (AMITIS) to accurately capture the coupled plasma and induced response self-consistently [5].

In order to fully characterize the plasma current systems, we compare two runs of the hybrid model: one with and one without a conductivity structure within the Moon. The first captures the coupled induced-plasma response. The second model captures the plasma current systems only. The residual of these two

runs can be subtracted from the downstream signal removing the non-geophysical (i.e., plasma) component of the signal. The remaining signal is fit with the geophysical induction model in order to constrain the electrical conductivity of the lunar interior.

Geophysical Forward Models: The global electromagnetic induction response of the Moon in a vacuum is solved for a variety of plausible homogeneous electrical conductivity models using the analytic expression developed by [1]. This model solves for the geophysically induced response in vacuum to a driving step transient event for a specified homogeneous conductivity profile.

Case Study: Figure 1 compares the magnetic field strength near and within the Moon as a function of time (columns) and conductivity structure (rows).

The model uses a right-handed coordinate system centered at the Moon, with the +X axis directed toward the Sun, which is the Selenographic Solar Ecliptic (SSE) coordinate system. Here, the solar wind flows along the -X axis. The simulation cell size is 100 km, and the lunar radius is $R_L=1,800$ km. The conducting lunar interior is modeled as $R_1 = 1,600$ km, σ_1 is as specified in the caption of Figures 1 and 2, surrounded with a resistive layer of 200 km and $1.0e-8$ S/m. The vacuum region is $1.0e-8$ S/m. The transient event is $\Delta B_{SSE} = [0, +1.5, +10]$ nT, and passes the Moon at $t = 30$ s. By the time $t = 59$ s, the event has completely passed the lunar sphere and telluric currents within the interior of the Moon remain. These currents diffuse into the Moon within the Cowling decay time dependent on the size and conductivity of the core layer.

Figure 2 displays the 3 component vector magnetic field time series in the RNE coordinate system (Radial is vertical up from the surface, North is aligned with the polar axis, and East points in that direction) for a single observation point at the anti-sub-solar point at the surface. The hybrid simulation is compared against the analytic model for each component for a lunar interior model of the same homogeneous conductivity and conducting radius. The Field difference (right column) displays the residual time series for the hybrid response of a conducting model (r10, $1e-3$ S/m, or r11, $1e-4$ S/m) minus the response of the resistive model (r12, $1e-8$ S/m). The analytic response plotted here consists only of the poloidal induced response only, and not the total field plotted in the left column.

XY,|B(t)|

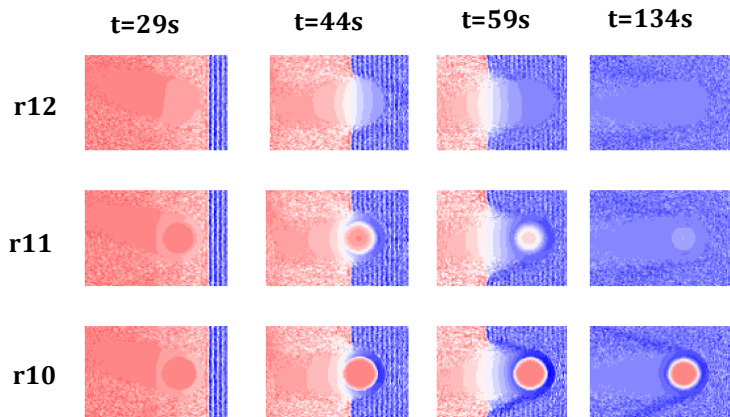


Figure 1. The time dependent magnetic field magnitude is shown for three varying lunar conductivities: purely resistive Moon r12 (1e-8 S/m), conducting Moon r11 (1e-4 S/m), and a highly conducting Moon r10 (1e-3 S/m). We note r12 provides the control demonstrating the wake fields only. The XY SSE plane is displayed from $+2R_m$ to $-4R_m$ in X and from $\pm 2R_m$ in Y. The color indicates the magnitude of the magnetic field where red = 26 nT, white = 16 nT, blue = 6 nT.

due to the coupling occurring between the induced and wake fields.

We conclude, for this case study, the effect of the diamagnetic wake currents is longer than the geophysical induction only. Thus, full characterization of the wake fields is required in conjunction with the induction story.

Future Work. Given the 3D orientation variability coupled with the large range of conditions seen within the lunar plasma environment, we characterize the environment one case at a time. Additional solar wind cases will be considered to generalize method improvements.

References: [1] P. Dyal and C.W. Parkin (1971) *JGR*, 76(25), 5947–5969. [2] Grimm and DeLory (2011) *Advances in Space Research*, 50(12), 1687–1701. [3] Fatemi et al. (2013) *GRL*, 40, 17-21. [4] Fatemi et al. (2015) *GRL*, 42, 6931-6938. [5] Fatemi et al. (2017) *J. of Physics: Conf. Ser.*, 837, 012017.

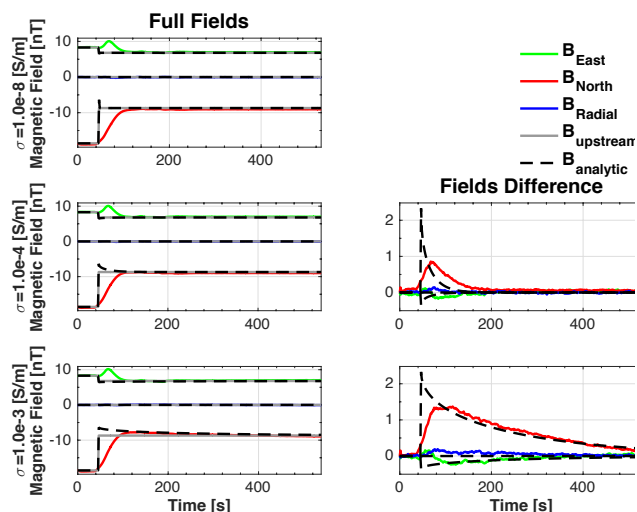


Figure 2. Observing Location 0: Anti-subsolar point $(-1, 0, 0) R_m$. In the RNE coordinate system, the total response observed is shown (left) and the difference between the conducting cases and the resistive case is shown (right). The upstream observer driving the induced response is shown in grey. The analytic response is shown for all three components, black dashed. Some aspects of the analytic induced response can be accounted for by removing the wake fields; however, not its entirety